**iScience, Volume *25***

## Supplemental information

# RBD trimer mRNA vaccine elicits broad and protective immune responses against SARS-CoV-2 variants

**Qingtai Liang, Yifeng Wang, Shuyuan Zhang, Jing Sun, Wenbo Sun, Jizhou Li, Yaping Liu, Mingxi Li, Lin Cheng, Yuhang Jiang, Ruoke Wang, Rui Zhang, Zihan Yang, Yifei Ren, Peng Chen, Peng Gao, Huayuan Yan, Zheng Zhang, Qi Zhang, Xuanling Shi, Jianbin Wang, Wanli Liu, Xinquan Wang, Bo Ying, Jincun Zhao, Hai Qi, and Linqi Zhang**

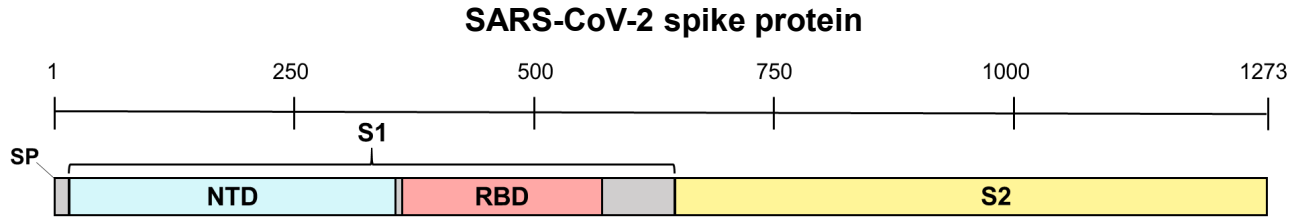


## Naturally occurring variants by strain

| Name \ Position | 5 | 13 | 18 | 19 | 20 | 26 | 52 | 67 | 69 | 70 | 80 | 95 | 138 | 142 | 144 | 152 | 154 | 156 | 157 | 158 | 190 | 215 | 242 | 243 | 244 | 253 | 305 | 367 | 417 | 452 | 478 | 484 | 501 | 570 | 613 | 614 | 655 | 677 | 681 | 701 | 716 | 888 | 950 | 982 | 1027 | 1071 | 1118 | 1176 |
|---|---|---|---|---|---|---|---|---|---|---|---|---|---|---|---|---|---|---|---|---|---|---|---|---|---|---|---|---|---|---|---|---|---|---|---|---|---|---|---|---|---|---|---|---|---|---|---|---|
| Wide type | L | S | L | T | T | P | Q | A | H | V | D | T | D | G | Y | W | E | E | F | R | R | D | L | A | L | D | S | V | K | L | T | E | N | A | Q | D | H | Q | P | A | T | F | D | S | T | Q | D | V |
| D614G | . | . | . | . | . | . | . | . | . | . | . | . | . | . | . | . | . | . | . | . | . | . | . | . | . | . | . | . | . | . | . | . | . | . | . | G | . | . | . | . | . | . | . | . | . | . | . | . | . | . |
| B.1.1.7 (Alpha) | . | . | . | . | . | . | . | . | - | - | . | . | . | . | - | . | . | . | . | . | . | . | . | . | . | . | . | . | . | . | . | . | Y | D | . | G | . | . | H | . | I | . | . | A | . | . | H | . |
| B.1.351 (Beta) | . | . | F | . | . | . | . | . | . | . | A | . | . | . | . | . | . | . | . | . | . | G | - | - | - | . | T | . | N | . | . | K | Y | . | . | G | . | . | . | V | . | . | . | . | . | . | . | . |
| P.1 (Gamma) | . | . | F | . | N | S | . | . | . | . | . | . | Y | . | . | . | . | . | . | . | S | . | . | . | . | . | . | . | T | . | . | K | Y | . | . | G | Y | . | . | . | . | . | . | . | . | I | . | . | F |
| B.1.617.2 (Delta) | . | . | . | R | . | . | . | . | . | . | . | . | . | . | . | . | . | - | - | G | . | . | . | . | . | . | . | . | . | R | K | . | . | . | . | G | . | . | R | . | . | . | N | . | . | . | . | . |
| B.1.617.1 (Kappa) | . | . | . | . | . | . | . | . | . | . | . | I | . | D | . | . | L | . | . | . | . | . | . | . | . | . | . | . | . | R | . | Q | . | . | . | G | . | . | R | . | . | . | . | . | . | H | . | . |
| B.1.526 (Lota) | F | . | . | . | . | . | . | . | . | . | . | I | . | . | . | . | . | . | . | . | . | . | . | . | . | G | . | . | . | . | . | K | . | . | . | G | . | . | . | Y | . | . | . | . | . | . | . | . | . |
| B.1.429 (Epsilon) | . | I | . | . | . | . | . | . | . | . | . | . | . | . | . | C | . | . | . | . | . | . | . | . | . | . | . | . | . | R | . | . | . | . | . | G | . | . | . | . | . | . | . | . | . | . | . | . | . |
| A23.1 | . | . | . | . | . | . | . | . | . | . | . | I | . | . | . | . | . | . | L | . | . | . | . | . | . | G | . | F | . | . | . | K | . | . | H | . | . | R | Y | . | . | . | . | . | . | . | . | . |
| B.1.525 (Eta) | . | . | . | . | . | . | R | V | - | - | . | . | . | . | - | . | . | . | . | . | . | . | . | . | . | . | . | . | . | . | . | K | . | . | . | G | . | H | . | . | . | L | . | . | . | . | . | . |

**Figure S1.**

**Schematic of SARS-CoV-2 spike protein structure and the mutation landscape of variants used in this study are illustrated, related to Figure 2, 5B.** SP, signal peptide; TM, transmembrane domain; RBD, receptor binding domain. In the mutation map, a dot (·) indicates the same amino acid in that position as wild type and a dash (–) indicates a deletion.

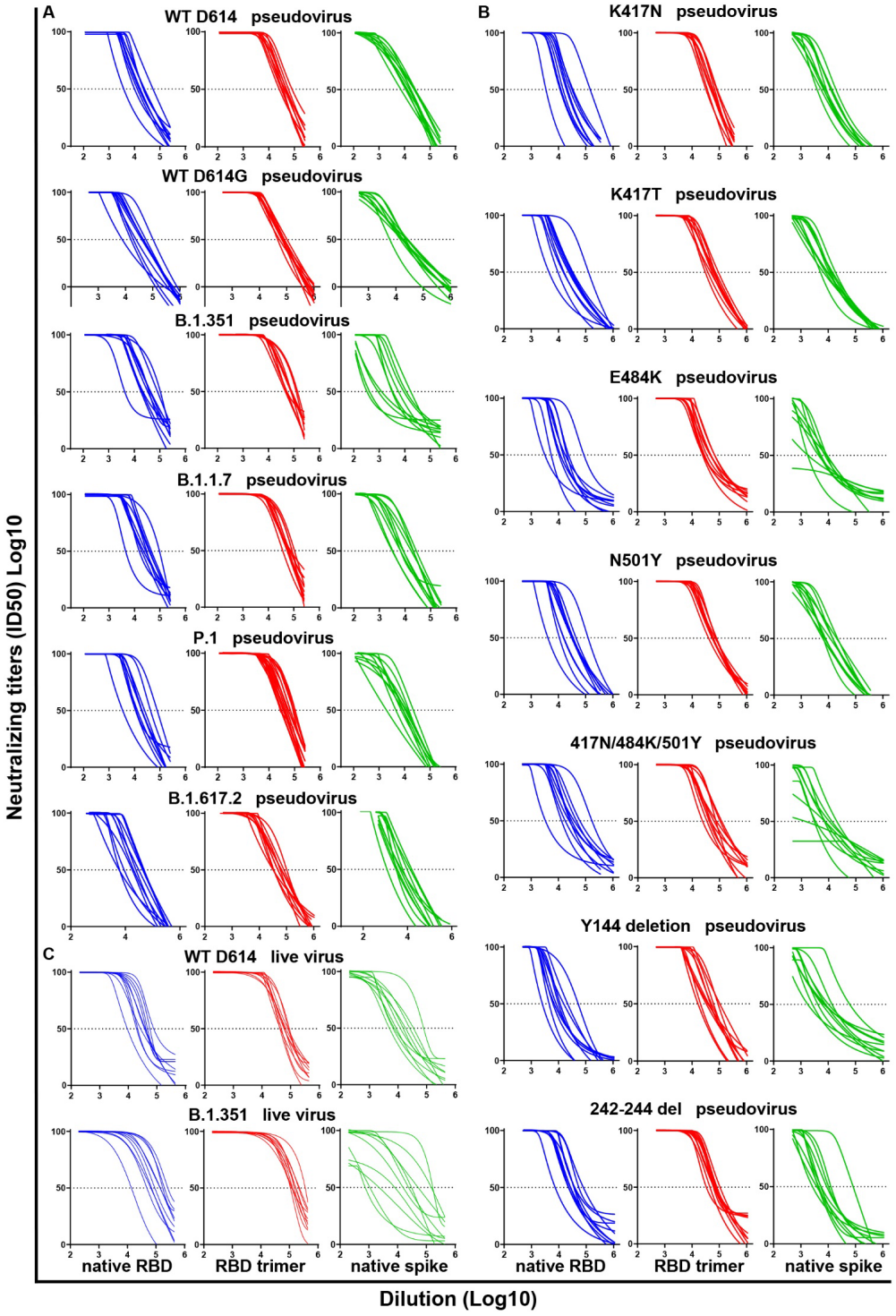


**Figure S2.**

**Serum neutralization of SARS-CoV-2 variants induced by the three mRNA vaccines, related to Figure 2.** Pseudoviruses bearing full-length, single, or triple mutant spike of SARS-CoV-2 variants (A, B) or live WT D614 and B.1.351 viruses (C) were tested against serial dilutions of immune serum. Neutralizing activity was defined as the percent reduction in luciferase activities or in plaque formation compared to no antibody controls. Fold change in reciprocal serum neutralization were calculated relative to that of WT D614G. Results shown are representative of two independent experiments. Dashed lines indicate 50% reduction in viral infectivity.

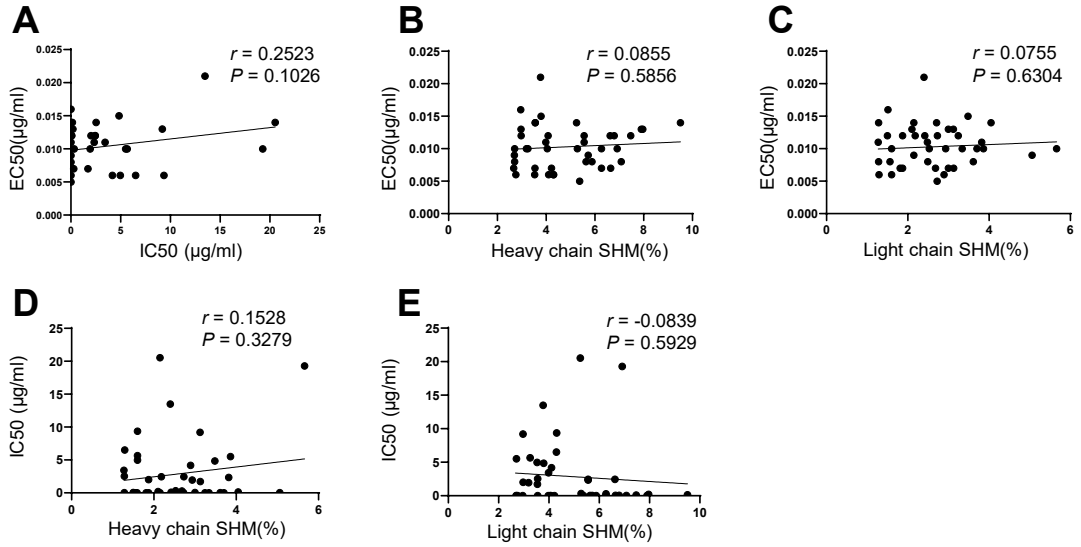


**Figure S3.**

**Relationship between IC50, EC50 and somatic hyper mutation of 43 isolated monoclonal antibodies, related to Figure 5A.** (A) Relationship between IC50 and EC50. n=43. (B) Relationship between EC50 and degree of heavy chains' somatic hyper mutation. n=43. (C) Relationship between EC50 and degree of light chains' somatic hyper mutation. n=43. (D) Relationship between IC50 and degree of heavy chains' somatic hyper mutation. n=43. (E) Relationship between IC50 and degree of light chains' somatic hyper mutation. n=43. (A-E) Simple linear regressions are shown with Pearson correlation (r) and P value (P).

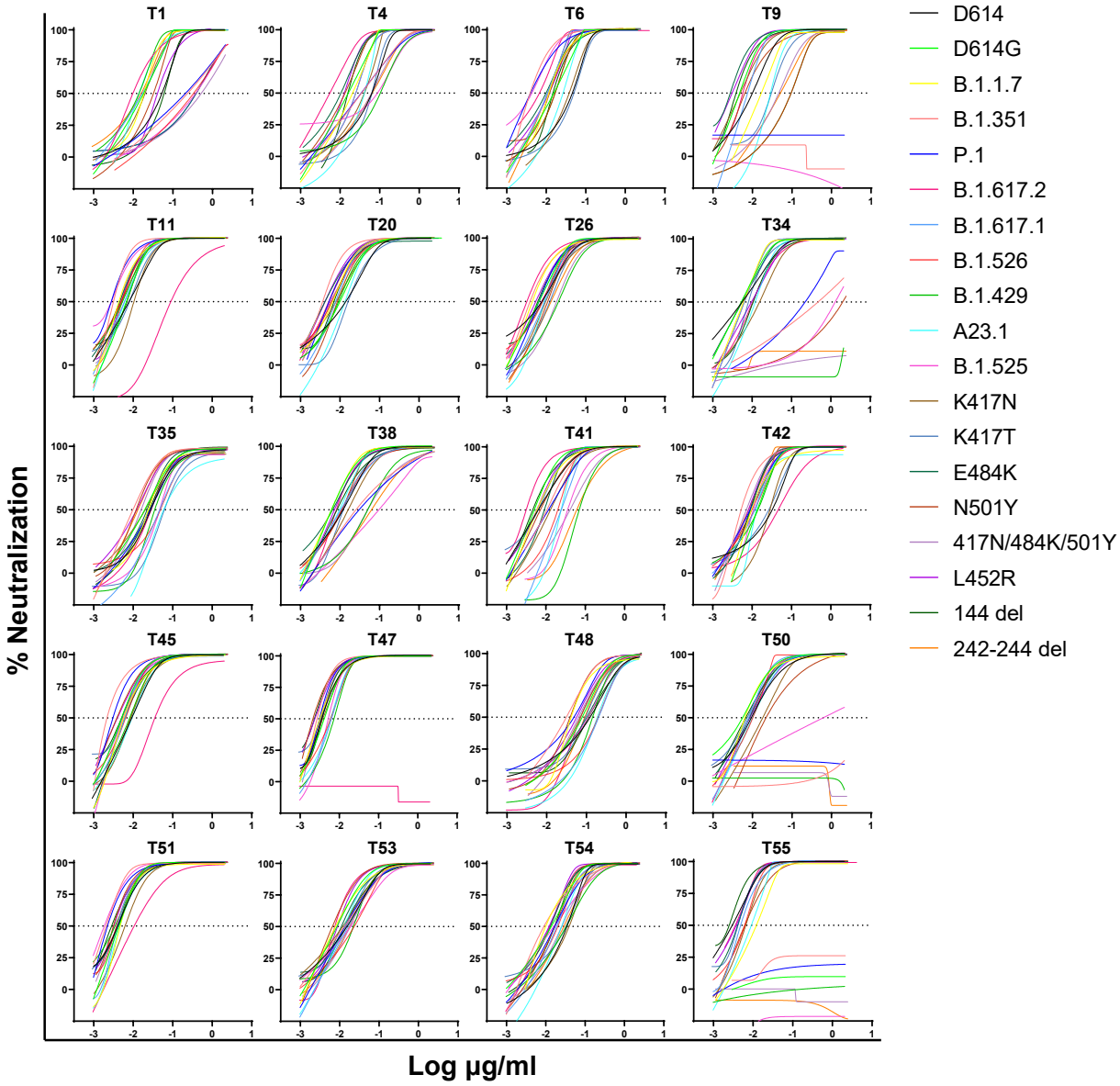


**Figure S4.**

**Neutralization of SARS-CoV-2 variants by each antibody, related to Figure 5B.** Pseudoviruses bearing the indicated mutations were tested against serial dilutions of each mAb. Neutralizing activity was defined as the percent reduction in luciferase activities compared to no antibody controls. Levels of resistance were calculated as the fold change in IC50 between each mutant and WT D614G, as presented in Figure 5B. Results were calculated from three independent experiments.

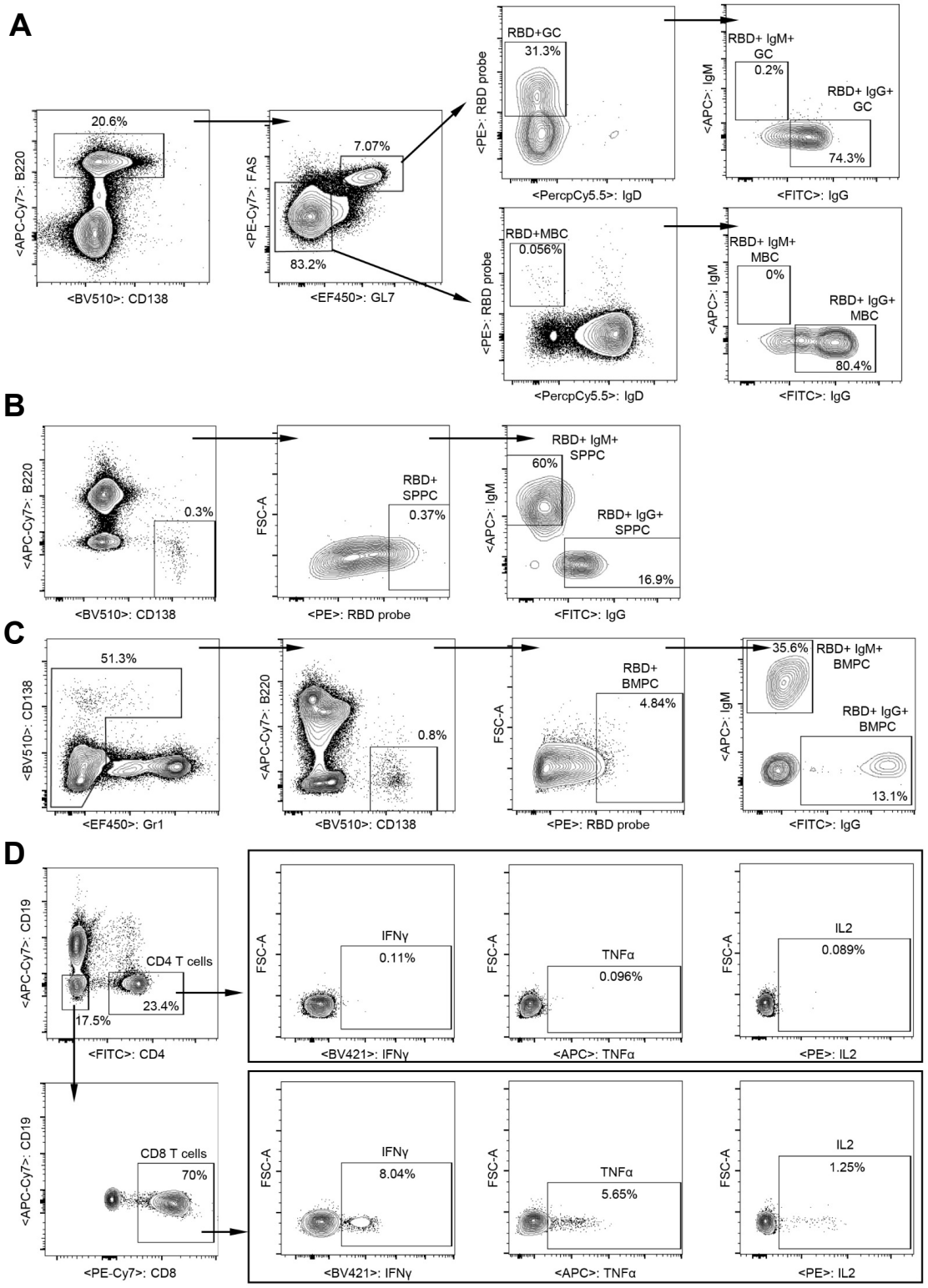


**Figure S5.**

**Gating strategy for and surface marker staining in B cells and intracellular cytokine staining in CD8+ and CD4+ T cells, related to Figure 3.** (A) Flow cytometric gating strategy for splenic RBD-specific IgG+ GC and MBC is shown. Inguinal lymph nodes' cells responses were gated similarly. (B) Flow cytometric gating strategy for splenic RBD-specific IgG+ plasma cells. (C) Flow cytometric gating strategy for RBD-specific IgG+ plasma cells in bone marrow. (D) Intracellular cytokine gating strategy for splenic CD4+ and CD8+ T cells.

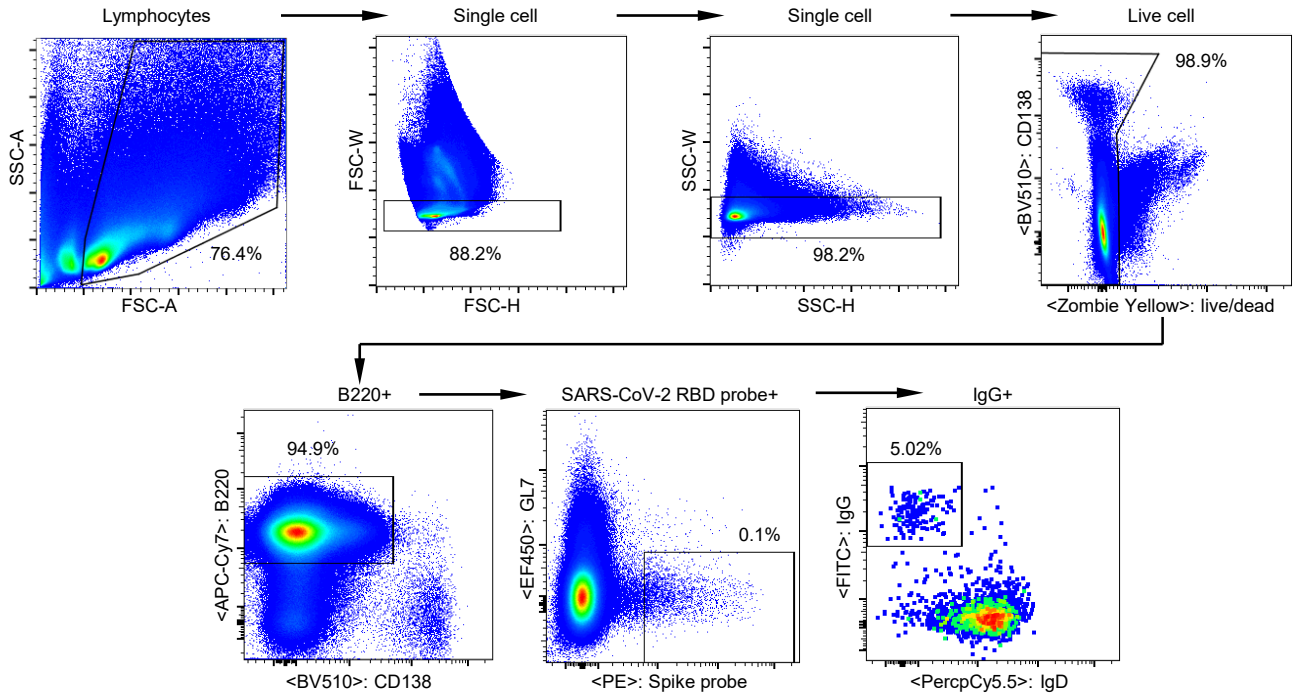


**Figure S6.**

**Gating strategy for isolation of Spike-specific memory B cells through FACS, related to Figure 5.** The isolated spike-specific IgG+ memory B cells from representative samples are highlighted in boxes with FITC fluorophores. FSC-W: forward scatter width. SSC-A: side scatter area.

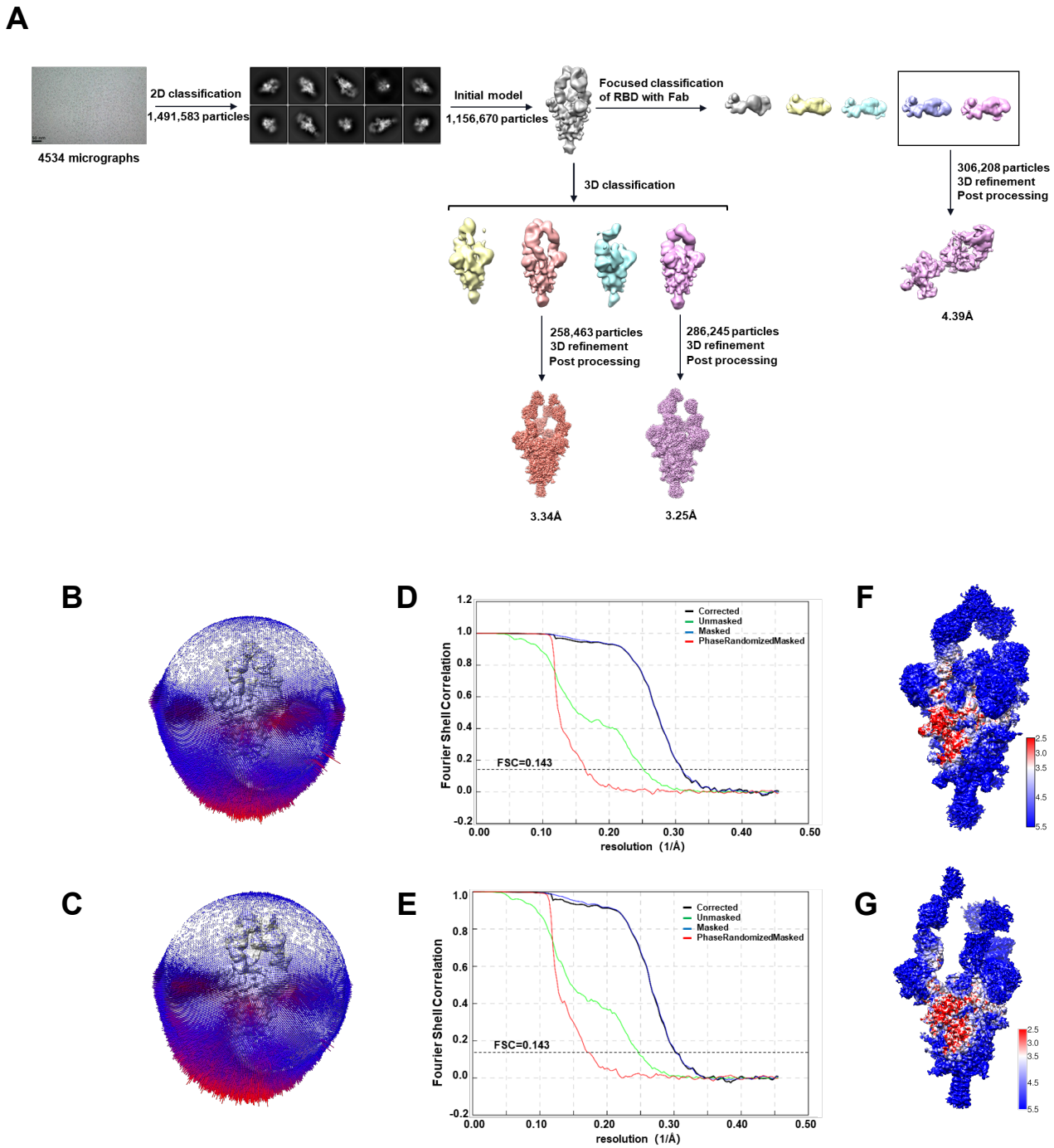


**Figure S7.**

**Cryo-EM structure validations, related to Figure 6A,6B.** (A) Processing schemes for cryo-EM data of SARS-CoV-2 spike trimer of B.1.351(SA) strain in a complex with mAb T6. (B, C) Particle orientation distribution in the final 3D reconstruction of the complex of SARS-CoV-2 spike trimer of B.1.351(SA) strain and mAb T6. (B) State1, two T6 Fabs bound with spike trimer. (C) State2, three T6 Fabs bound with spike trimer. (D, E) The corrected, unmasked, masked and phase randomized FSC for the cryo-EM reconstructions of the density maps of the complex. The final resolution of state1 (D) is 3.25 Å and state2 (E) is 3.34 Å. (F, G) Local resolution map of the overall complex. A color scale on the right indicates resolution (2.5-5.5 Å), (F) state 1, (G) state 2.